Biuletyn WAT
Vol. LXV, Nr 1, 2016

Numerical solution of reinforced concrete beam using arc-length method

PIOTR SMARZEWSKI

Lublin University of Technology, Faculty of Civil Engineering and Architecture,
40 Nadbystrzycka Str., 20-618 Lublin, Poland, p.smarzewski@pollub.pl

Abstract. This article discusses numerical solution of a reinforced concrete beam. The modelling was conducted with the rules of the finite element method (FEM). In order to verify the correctness of the assumed material's models: concrete and reinforcing steel, the results obtained with the arc-length method finite analysis were compared with experimental data. The method had been verified in the beam spatial model, in which concrete crushing at compressive and concrete stiffening at tensile are dominant phenomena. The arc-length method is the only one to offer the possibility of obtaining a complete load-deflection curve with local and global softening.
Keywords: mechanics of concrete structures, finite element method, reinforced concrete beam, arc-length algorithm
DOI: 10.5604/12345865.1197966

1. Introduction

There are a number of methods for modelling reinforced concrete members for both analytical and numerical approaches. The finite element method (FEM) is applied to analyse reinforced concrete structures based on the use of non-linear behaviour of the materials. The FEM simulations can provide the response of reinforced concrete members. The use of FEM has increased due to the advancement of knowledge and capabilities of computer software and hardware. The non-linear material models are integrated in numerous of purpose of FE codes: MSC NASTRAN, ABAQUS, ADINA or ANSYS. The literature provides many studies in which there were modelled the reinforced concrete members. Kachlakev et al. [1] studied the beams externally strengthened with

reinforced plastic carbon fiber with no stirrups. Wolanski [2] used the ANSYS program to study the flexural failure of reinforced and prestressed concrete beams. Smarzewski and Stolarski [3] and Smarzewski [4] studied the flexural failure of reinforced concrete and high-strength concrete beams by using ANSYS. Özcan et al. [5] investigated the steel fiber reinforced concrete beam by using non-linear material properties till the ultimate failure cracks by ANSYS. Korol and Tejchman [6] used the ABAQUS program to study the size effect in concrete and reinforced concrete beams. An elasto-plastic model with non-local softening was used. The non-linear analysis was applied to investigate the shear failure in tensile reinforced concrete beams without stirrups by Słowik and Smarzewski [7, 8]. Szcześniak and Stolarski [9] studied the effort of reinforced concrete beams using dynamic relaxation.

In this study, the simulation of reinforced concrete beam behaviour was performed by using the ANSYS program. An analysis of the reinforced concrete beam, modelled as a concrete member with discreetly distributed steel rebars, is conducted. The failure modes of reinforced concrete beam under static load, with the consideration for physical non-linearity and for geometrical non-linearity, are modelled. A concrete model for elastic-plastic material, with the consideration for softening in compression and tension, was applied. The finite analyses in the range of static large displacement were considered. The static equilibrium equation using arc-length method was solved. Numerical results were compared with experimental data described by Buckhouse [10].

2. Modelling of concrete and steel reinforcement

The concrete failure surface was presented with a five-parameter William and Warnke model [11]. On the basis of experimental data [12, 13] and modification of the dynamic strength criterion [14, 15], stress-strain relation for the concrete with elastic-plastic hardening and the material softening in the uniaxial compression was applied. Point no 1, defined as 33% of the ultimate compressive strength f_c is calculated in the linear range. Also for the range of elastic-plastic concrete hardening linear increase to f_c was accepted. In the third range of concrete softening, stress down to 80% of f_c at ultimate strain ε_{cu} was assumed. The strains $\varepsilon_{c1} = 6‰$ and $\varepsilon_{cu} = 12‰$ were adopted. The stress-strain curve in uniaxial tension is linear up to the ultimate tensile strength f_t. On the basis of paper [16], the equality of concrete modulus elasticity for compression and concrete modulus elasticity for tension were considered. After reaching f_t there is a brittle fracturing of the material and strength decreases down to 40%.

Bilinear isotropic model for all types of the steel reinforcement is assumed. The bilinear isotropic material is based on the Mises failure criteria. This model

requires the yield strength and hardening modulus to be defined. Linear isotropic model for the steel plates at support and loading point was assumed.

3. Method of analysis

3.1. Model of reinforced concrete beam

The FEA modelling a concrete beam was performed using ANSYS. In the finite analysis of reinforced concrete beam the dimensions, reinforcement arrangement, load scheme and material properties corresponding to C1-beam tested by [10] were used. The test setup is presented in Fig. 1.

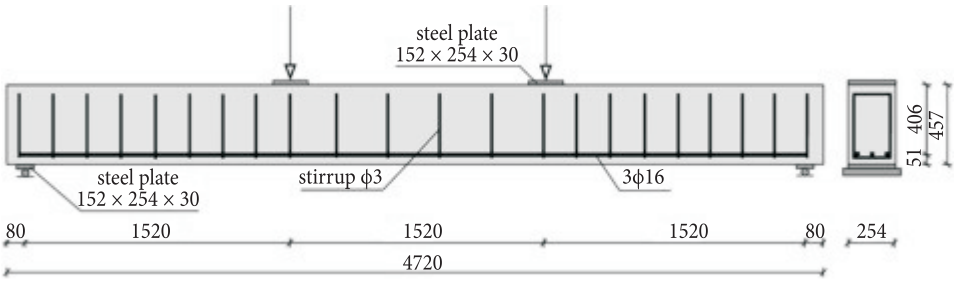

Fig. 1. Test setup (all dimensions are in mm)

Concrete control C1-beam was performed with flexural and shear reinforcement. Stirrups were placed to force a flexural failure mechanism. A beam was loaded with transverse point loads at two points along the beam. Loading was applied to the beam until failure occurred. The linear variable displacement transformer (LVDT) was used to measure the deflection at mid-span. The measuring device was put on the beam after it was set in the test fixture. Deflections were taken relative to a zero deflection point after the self-weight was introduced.

Stress-strain parameters assumed for the concrete and steel were described in paper [17]. Due to the symmetry of the element, a one quarter of beam, sized 2360 mm × 457 mm × 127 mm, was modelled. To obtain correct results, the rectangular mesh was used. The discrete model of the reinforcement was used. No mesh of the reinforcement was needed because rebars elements were made through the concrete mesh nodes. A perfect bond between the concrete and steel reinforcement was considered. In this study, the steel link elements were connected between nodes of adjacent concrete solid elements, so these materials shared the same nodes. The tensile rebars also shared the same nodes as the stirrups. The width and length in the steel plates at support and loading point consistent with the elements

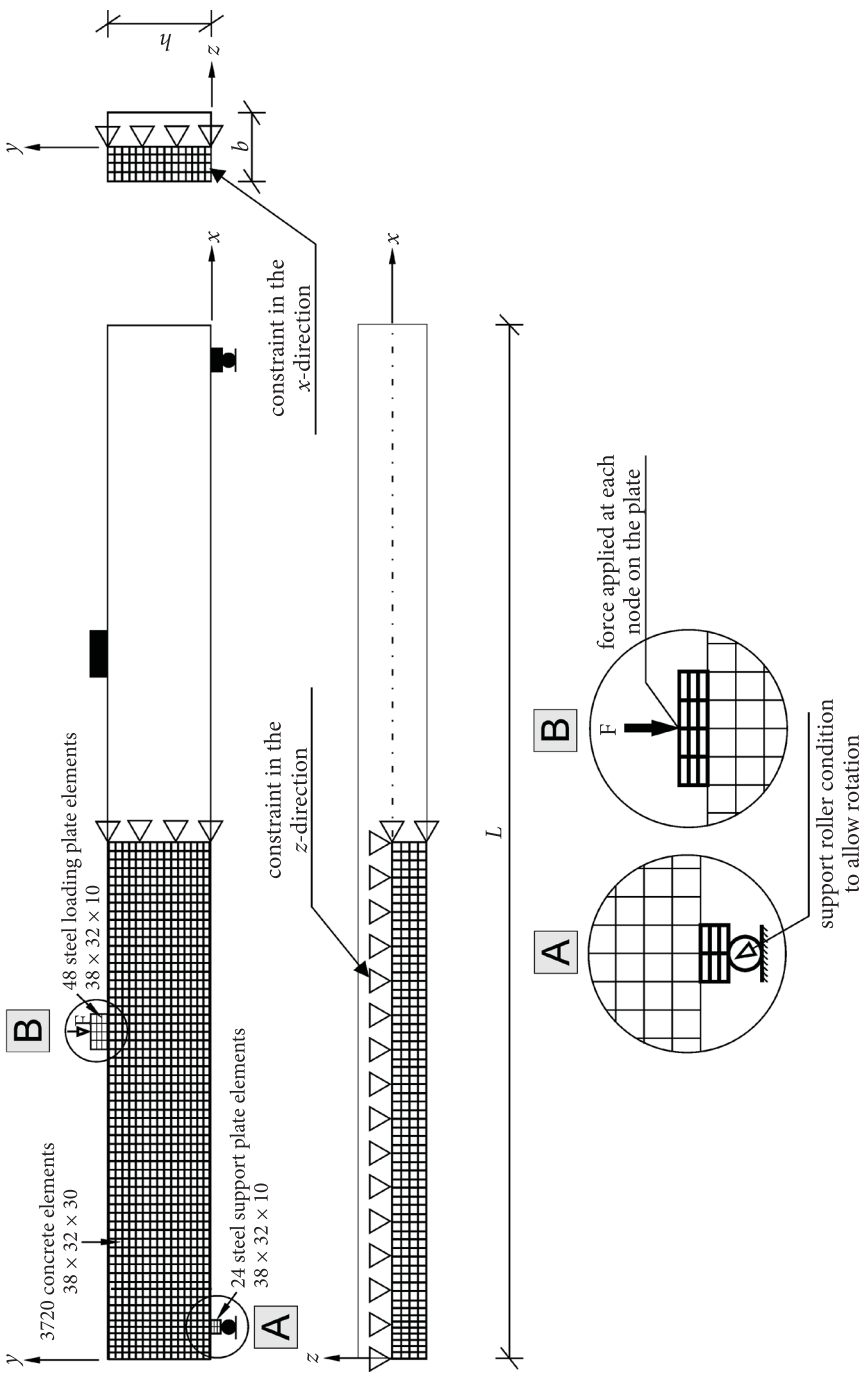

Fig. 2. Mesh and boundary conditions for one quarter of C1-beam (unit in mm)

and nodes in the concrete elements was set. Figure 2 presents the mesh, boundary conditions in the symmetry plains, boundary conditions on the support and loading plate and statistical description of the numerical model.

The link element to model steel rebars was used. This element is a spatial spar element. It has two nodes with three degrees two nodes with three degrees of freedom (translations) in each of them. This element is capable of plastic deformation. The modulus of elasticity and yield stress for the steel reinforcement was used to follow the material properties used in experimental research. The model of elastic--perfectly plastic material with identical properties in tension and compression for steel reinforcement was assumed. A Poisson's ratio of 0.3 was used.

The solid element was used for the steel plates at support and loading point in order to avoid stress concentration problems. The modulus of elasticity equal to 200 MPa and Poisson's ratio of 0.3 were used for the plates. The steel plates were assumed to be linear elastic materials. The support was modelled in such a way that a roller, allowing the beam to rotate, was created. Nods located in the middle of the support plate were given constraint in the x and z directions. The force was applied across the entire centreline of the loading plate.

3.2. Arc-length method

The arc-length method in the structure finite analysis was used by Wempner [18], Bergan et al. [19], and Riks [20]. Crisfield [21-23], Ramm [24], Forde and Stiemer [25], Belleni and Chulya [26], and Lam and Morley [27] made further modifications for this method. More information is provided by Crisfield [28] and Memon and Su [29].

The arc-length method is shown in Fig. 3. In this algorithm, Newton-Raphson equation is dependent on the load parameter λ:

$$\left[K_i^T\right]\left\{\Delta u_i\right\} = \lambda\left\{F^a\right\} - \left\{F_i^{nr}\right\}, \tag{1}$$

where: $[K_i^T]$ — tangent stiffness matrix;
i — subscript representing the equilibrium iteration;
$\{F_i^{nr}\}$ — vector of restoring load corresponding to the element's internal load;
$\{F^a\}$ — vector of applied load.

In this procedure, the total load parameter λ is determined from the equilibrium equations in the procedure of finite element from the range $-1 \leq \lambda \leq 1$. In the incremental substep, the equation has the following form:

$$\left[K_i^T\right]\left\{\Delta u_i\right\} - \Delta\lambda\left\{F^a\right\} = \left(\lambda_0 + \Delta\lambda_i\right)\left\{F^a\right\} - \left\{F_i^{nr}\right\}, \tag{2}$$

in which: $\Delta\lambda$ — incremental load parameter.

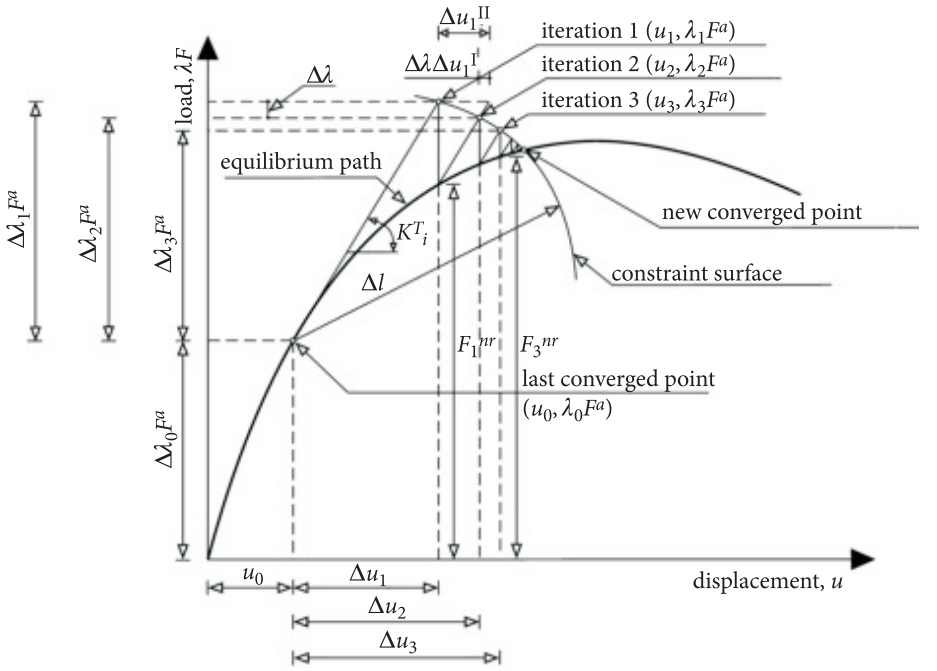

Fig. 3. Arc-length method [22]

On the basis of Eq. (2), the vector of incremental displacement $\{\Delta u_i\}$ consists of two components described as:

$$\left\{\Delta u_i\right\} = \Delta\lambda\left\{\Delta u_i^I\right\} + \left\{\Delta u_i^{II}\right\}, \tag{3}$$

where: $\{\Delta u_i^I\}$ — vector of displacement increment caused by a unit load parameter;
$\{\Delta u_i^{II}\}$ — vector of displacement increment in the Newton-Raphson method.

Displacement vectors are defined as:

$$\left\{\Delta u_i^I\right\} = \left[K_i^T\right]^{-1}\left\{F^a\right\}, \tag{4}$$

$$\left\{\Delta u_i^{II}\right\} = \left[K_i^T\right]^{-1}\left[\left(\lambda_0 + \Delta\lambda_i\right)\left\{F^a\right\} - \left\{F_i^{nr}\right\}\right]. \tag{5}$$

The incremental load parameter $\Delta\lambda$ is defined from the arc-length equation:

$$l_i^2 = \Delta\lambda_i^2 + \beta^2\left\{\Delta u_n\right\}^T\left\{\Delta u_n\right\}, \tag{6}$$

where: β — scaling factor;
Δu_n — the sum of all displacement increments Δu_i in the current iteration step.

There are many ways of calculating approximate $\Delta\lambda$. Work [23] presents a general procedure of computing the parameter $\Delta\lambda$ ensuring orthogonality:

$$\Delta\lambda = \frac{r_i - \{\Delta u_n\}^T \{\Delta u_i^{II}\}}{\beta^2 \Delta\lambda_i + \{\Delta u_n\}^T \{\Delta u_i^{I}\}}, \tag{7}$$

where: r_i — required residual for explicit iteration on a sphere.

The final vectors are updated according to:

$$\{u_{i+1}\} = \{u_0\} + \{\Delta u_n\} + \{\Delta u_i\}, \tag{8}$$

$$\lambda_{n+1} = \lambda_0 + \Delta\lambda_i + \Delta\lambda, \tag{9}$$

n — current substep number.

Iterations stop at the moment of obtaining the convergence of the numerical solution.

In this study, the convergence criteria were based on force and displacement. The convergence tolerance limits were initially selected by the ANSYS program. Convergence of solutions for the model beam was difficult to achieve due to the non-linear behaviour of reinforced concrete. Thus, the convergence limits were increased to maximum 5 times the default tolerance limits (0.5% for force checking and 5% for displacement checking) in order to obtain convergence of the solution.

4. Results and discussion

4.1. Cracking propagation analysis

Both cracking and crushing failure modes are accounted for concrete. In the concrete element, cracking occurs when the principal tensile stress in any directions lies outside the failure surface. After cracking, the elastic modulus of the concrete is set to zero in the direction parallel to the principal tensile stress direction. Crushing occurs when all principal stresses are compressive and lie outside the failure surface. Subsequently, the element effectively disappears. The ANSYS program records a crack pattern at each applied load step. Cracking is shown with a circle outline in the plane of the crack. Crushing is shown with an octahedron

outline. The first, second, and third crack at an integration point are shown with red circle outline, green circle outline, and blue circle outline, respectively.

The smeared cracks' patterns obtained at different levels of the load are presented in Fig. 4.

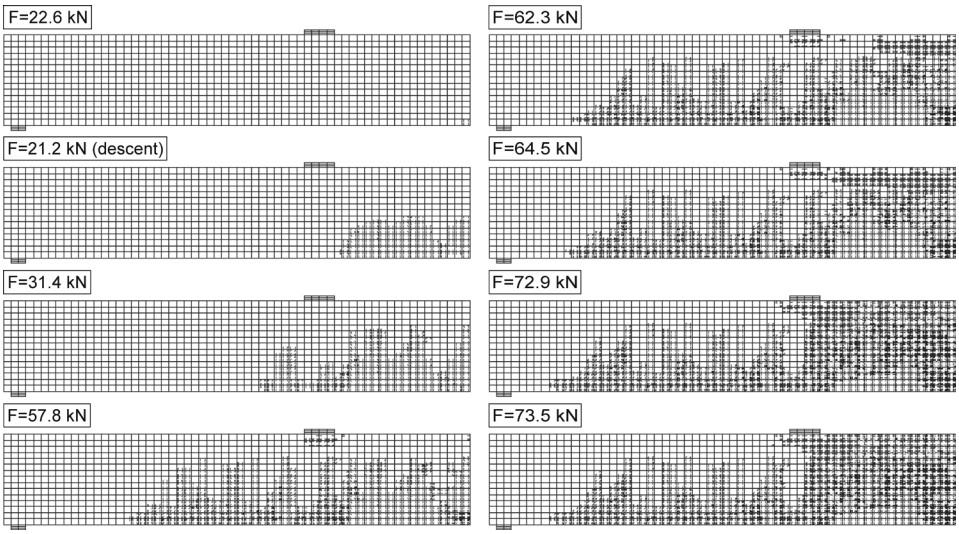

Fig. 4. Evolution of crack patterns

Initially, flexural cracks propagate in the constant moment region in the beam mid-span, up to the load of 22.6 kN. Further cracks grow horizontally towards the support. Significant cracking occurs at 57.8 kN. The cracks from crushing concrete under the loading plate and diagonal tension cracks at the mid-shear-span are occurred. Yielding of steel reinforcement at 62.4 kN is appeared. Further development of the flexural cracks and diagonal cracks is observed. At the last converged load steps, numerous compressive cracks occur at the top part of the beam, and many flexural cracks are observed at mid-span as well.

4.2. Strain and stress analysis

In order to control the concrete strain data under loading, the point placed on the top face of the beam was selected. The tensile strain results for steel reinforcement were recorded in longitudinal rebar at the beam mid-span. Figure 5a shows the load-strain plot for the concrete from the finite element analysis at the mid-span of C1-beam, whereas Fig. 5b presents the load-strain plot for the tensile steel rebar at mid-span. In both curves, one can see an insignificant force descent at the first cracking load.

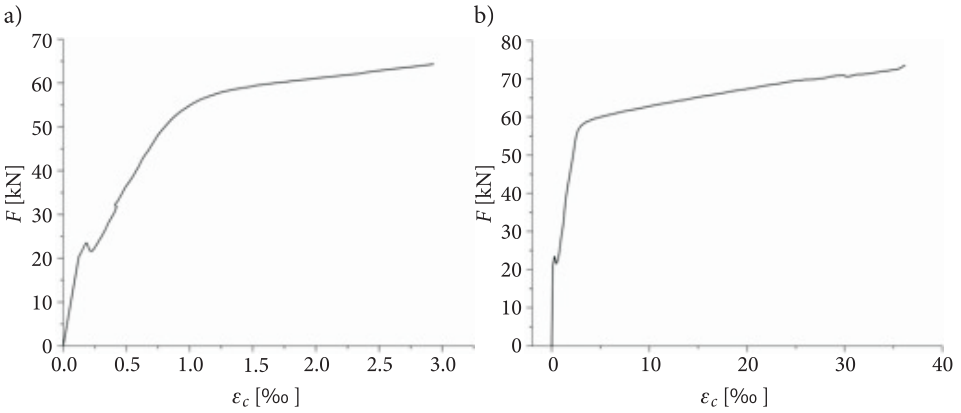

Fig. 5. Load-strain plots for (a) compressive concrete; (b) tensile steel rebar

Other images concern non-elastic behaviour of the concrete under static loading. Figure 6 shows the normal stresses for the model C1-beam. At the load of $F = 22.6$ kN, the first plasticity stress in the tension part of the concrete beam in the constant moment region can be observed. In this tension area, the concrete beam is initially plasticised at the first cracking load. In the remaining part of the beam, the concrete works within the elastic range for tension and compression.

Further loading causes that in the flexural concrete the sudden cracking occurs. This results in a decrease in force down to $F = 21.2$ kN. Nearby cracking zone, an increase in the plasticity stress towards the support can be observed. At the load of $F = 62.3$ kN one can see the connection of the cracking zone with the plasticity area. Further development of concrete plasticity area for compression in the region of constant moment is also observable. At $F = 68.9$ kN, this caused the transition in the top face of the beam to the material softening. Exceeding the load capacity of a beam is caused by the local crushing of concrete at the mid-span, similar to the experimental beam [10]. With increase in load, the approximation of neutral axis to the top face of the beam can be seen. In Ia-phase, the neutral axis is located below the central axis of the beam. In subsequent phases, it adopts increasingly high positions. At the failure load, neutral axis is located close to the top face of the beam. This is the region where cracks run through the significant part of the cross-section. For large cross-sectional areas of steel reinforcement, neutral axis does not rise so high and frequently does not even reach the central axis of the beam. The neutral axis moves away from the top face of the beam.

These stresses are similar to the distribution of stresses obtained in Newton-Raphson method using adaptive descent. The tensile normal stresses σ_x and the compressive tangent stresses σ_{xy} determine the diagonal direction of the principal stresses. They cause the formation of diagonal tensile cracks in the shear-span.

On the other hand, the tensile tangent stresses σ_{yz} and σ_{xz} contribute to the development of concrete flexural cracks in the constant moment region.

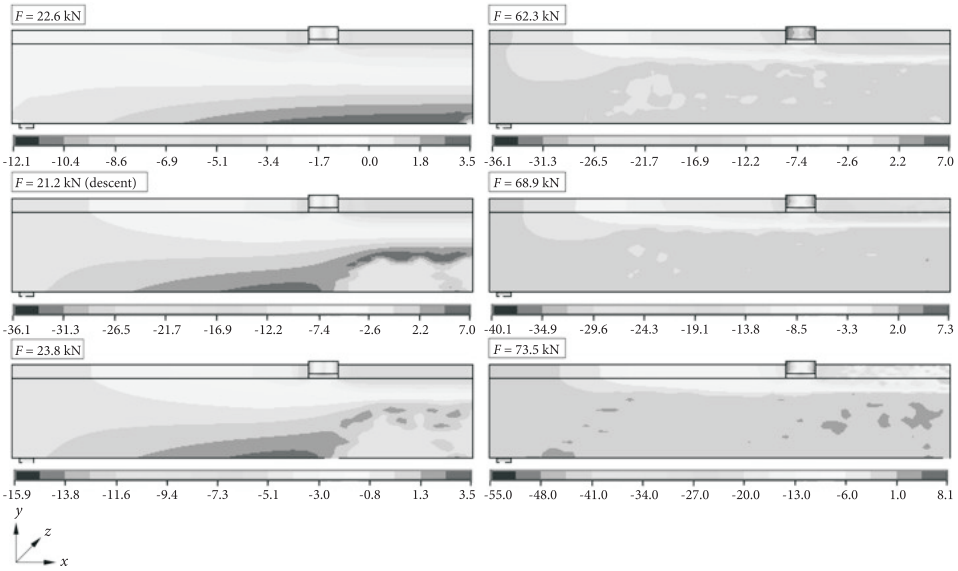

Fig. 6. Normal stress σ_x under loading (unit in MPa)

4.3. Load-deflection curves analysis

Curves of load-defection at the lower edge of the beam ($F - u_d$) are non-monotonous due to the assumed concrete model with softening in the process of deformation. Obtaining a complete computational path with local decrease in stiffness (at the first cracking load) and global softening (at the crushing load) is possible by using the arc-length method. It was indicated that the patterns of crack in the tension region are not compensated by elastic steel reinforcement properties and by concrete plasticity at the top edge of the beam [30]. These instabilities can be seen on the load-deflection curve as sudden decrease in load. Therefore, it is justified to use the methods which allow us to reflect the effects of concrete softening. In both, the region of elastic stresses and after cracking, the model beam is characterised by the higher stiffness than the experimental beam. The increase in stiffness is connected with the changes of modulus of elasticity for cracking concrete and with the assumption of perfect bond between steel rebars and concrete. The ultimate deflection at beam mid-span of 92.72 mm from the model is approximately equal to the experimental ultimate deflection of 92.7 mm. The load-deflection plot from the FEA agrees excellent with the experimental data for the C1-beam (see Fig. 7).

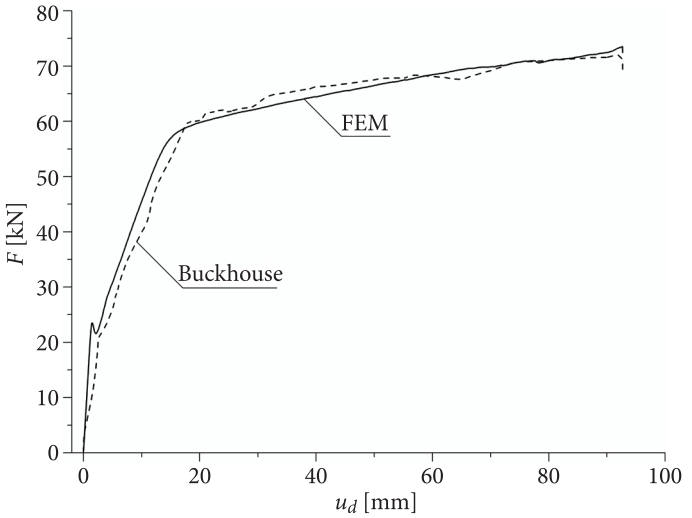

Fig. 7. Load-deflection plot for C1-beam

Figure 8 shows that the load-deflection curves for the C1-beam form the experimental data and the finite element analyses are in reasonably good agreement.

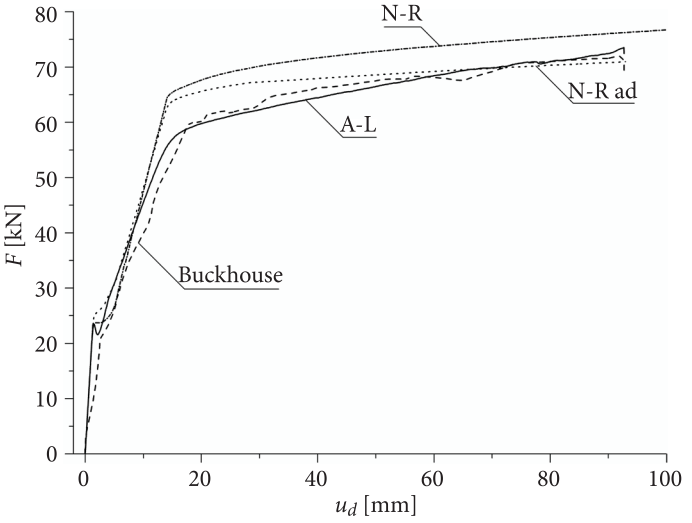

Fig. 8. Load-deflection curves for C1-beam obtained using different algorithms

The failure load for the finite element model beam is $F = 72.6$ kN, which is higher than the ultimate load obtained with Newton-Raphson procedure using adaptive descent by 5% [17]. All the incremental-iterative algorithms: Newton-Raphson procedure (N-R), quasi-Newton procedure using adaptive descent (N-R ad), and arc-length procedure (A-L) have given acceptable numerical results.

Summary

The paper evaluates the effectiveness of FEM procedures in non-linear analysis of reinforced concrete beam modelled as a spatial structural member. The solution of static equations in the FEM was made on the basis of arc-length method. The method had been verified in the spatial models of reinforced concrete members with concrete crushing and stiffening.

On the basis of reinforced concrete beam under static load, a comparison of theoretical and experimental results was made. The comparison proved the correctness of the assumptions concerning the concrete and steel models, and numerical algorithms to solve non-linear equilibrium equations. The arc-length method gives the possibility of obtaining a complete solution path of load-deflection with local and global softening. Moreover, the algorithm is characterised by high efficiency. Load step increments and properly set arc-length parameters guarantee the shortening of time numerical computing, still with very precise data. The obtained results and conclusions can be the basis for further research on modelling the failure modes in the reinforced concrete members.

Received December 20, 2012. Revised October 26, 2015.

REFERENCES

[1] Kachlakev D.I., Miller T., Yim S., Chansawat K., Potsiuk T., *Finite Element Modeling of Reinforced Concrete Structures Strengthened with FRP Laminates*, California Polytechnic State University, May, 2001.

[2] Wolanski B.S., *Flexural Behavior of Reinforced and Prestressed Concrete Beams Using Finite Element Analysis*, Master's Thesis, Milwaukee, Wisconsin, May 2004.

[3] Smarzewski P., Stolarski A., *Modelowanie zachowania niesprężystej belki żelbetowej*, Biul. WAT, 56, 2, 2007, 147-166.

[4] Smarzewski P., *Analiza numeryczna niesprężystych belek żelbetowych z betonu wysokiej wytrzymałości o niskim stopniu zbrojenia*, Budownictwo i Architektura, 4, 2009, 5-30.

[5] Özcan D.M., Bayraktar A., Şahin A., Haktanir T., Türker T., *Experimental and finite element analysis on the steel fiber-reinforced concrete (SFRC) beams ultimate behavior*, Construction and Building Materials, 23, 2009, 1064-1077.

[6] Korol E., Tejchman J., *Experimental and theoretical studies on size effects in concrete and reinforced concrete beams*, CMM-2011 — Computer Methods in Mechanics, Warsaw, Poland, 9-12 May 2011.

[7] Słowik M., Smarzewski P., *Study of the scale effect on diagonal crack propagation in concrete beams*, Computational Materials Science, 64, 2012, 216-220.

[8] Słowik M., Smarzewski P., *Numerical modeling of diagonal cracks in concrete beams*, Archives of Civil Engineering, 60, 3, 2014, 307-322.

[9] Szcześniak A., Stolarski A., *Analiza wytężenia belek żelbetowych metodą relaksacji dynamicznej*, Inżynieria i Budownictwo, 5, 2012, 267-269.

[10] Buckhouse E.R., *External Flexural Reinforcement of Existing Reinforced Concrete Beams Using Bolted Steel Channels*, Master's Thesis, Marquette University, Milwaukee, Wisconsin, 1997.

[11] Willam K.J., Warnke E.P., *Constitutive Model for the Triaxial Behavior of Concrete*. International Association for Bridge and Structural Engineering, vol. 19, ISMES, Bergamo, Italy, 1975, 1-30.

[12] Pecce M., Fabbrocino G., *Plastic Rotation Capacity of Beams in Normal and High-Performance Concrete*, ACI Structural Journal, March-April 1999, 290-296.

[13] Kamińska M.E., *Doświadczalne badania żelbetowych elementów prętowych z betonu wysokiej wytrzymałości*, KILiW, PAN, Łódź, 1999.

[14] Stolarski A., *Model dynamicznego odkształcenia betonu*, Archiwum Inżynierii Lądowej, t. 37, z. 3-4, 1991, 405-447.

[15] Stolarski A., *Dynamic Strength Criterion for Concrete,* Journal of Engineering Mechanics, American Society of Civil Engineering, vol. 130, no 12, December 2004, 1428-1435.

[16] Lyndon F.D., Balendran R.V., *Some observations on elastic properties of plain concrete*, Cement and Concrete Research, 16, no 3, 1986, 314-324.

[17] Smarzewski P., *Numerical solution of reinforced concrete beam using Newton-Raphson method with adaptive descent*, Biuletyn WAT, 64, 4, 2015, 207-221.

[18] Wempner G.A., *Discrete approximation related to nonlinear theories of solids*, International Journal of Solids and Structures, 7, 1971, 1581-1599.

[19] Bergan P.G., Horrigmoe G., Krakeland B., Soreide T.H., *Solution techniques for nonlinear finite element problems*, International Journal for Numerical Methods in Engineering, 12, 1978, 1677-1696.

[20] Riks E., An *incremental approach to the solution of snapping and buckling problems*, International Journal of Solids and Structures, 15, 1979, 529-551.

[21] Crisfield M.A., A *fast incremental/iterative solution procedure that handles snap-through*, Computer and Structures, 13, 1981, 55-62.

[22] Crisfield M.A., *Variable Step-Length for Nonlinear Structural Analysis*, Report 1049, Transport and Road Research Lab., Crowthorne, England, 1982.

[23] Crisfield M.A., An *arc-length method including line searches and accelerations*, International Journal for Numerical Methods in Engineering, 19, 1983, 1269-1289.

[24] Ramm E., *Strategies for Tracing the Nonlinear Response near Limit Points*, Nonlinear Finite Element Analysis in Structural Mechanics, Springer, New York, 1981.

[25] Forde B.W.R., Stiemer S.F., *Improved arc length orthogonality methods for nonlinear finite element analysis*, Computers and Structures, 27, 1987, 625-630.

[26] Belleni P.X., Chulya A., An *improved automatic incremental algorithm for the efficient solution of nonlinear finite element equations*, Computers and Structures, 26, 1987, 99-110.

[27] Lam W.F., Morley C.T., *Arc-length method for passing limit points in structural calculation*, Journal of Structural Engineering, 118(1), 1992, 169-185.

[28] Crisfield M.A., *Non-linear Finite Element Analysis of Solids and Structures*, John Wiley & Sons, Inc., 2000.

[29] Memon B.A., Su X., *Arc-length technique for nonlinear finite element analysis*, Journal of Zhejiang University Science, 5, 2004, 618-628.

[30] Rashid M.A., Mansur M.A., *Reinforced High-Strength Concrete Beams in Flexure*, ACI Structural Journal, vol. 102, 3, May-June 2005, 462-471.

P. SMARZEWSKI

Rozwiązanie numeryczne belki żelbetowej metodą długości łuku

Streszczenie. W artykule przedstawiono rozwiązanie numeryczne belki żelbetowej. Modelowanie przeprowadzono z wykorzystaniem zasad metody elementów skończonych (MES). W celu zweryfikowania poprawności założonych modeli materiałów: betonu i stali zbrojeniowej, porównano otrzymane wyniki analizy numerycznej metodą długości łuku z wynikami doświadczalnymi. Metodę zweryfikowano na przestrzennym modelu belki, w którym decydującym zjawiskiem jest miażdżenie betonu przy ściskaniu i zesztywnienie przy rozciąganiu. Metoda długości łuku jako jedyna oferuje możliwość uzyskania kompletnej ścieżki obciążenie-ugięcie z lokalnym i globalnym osłabieniem.

Słowa kluczowe: mechanika konstrukcji betonowych, metoda elementów skończonych, belka żelbetowa, algorytm długości łuku

DOI: 10.5604/12345865.1197966